

# 000 001 002 003 004 005 006 007 008 009 010 011 012 013 014 015 016 017 018 019 020 021 022 023 024 025 026 027 028 029 030 031 032 033 034 035 036 037 038 039 040 041 042 043 044 045 046 047 048 049 050 051 052 053 SELF-REWARDING VISION-LANGUAGE MODEL VIA REASONING DECOMPOSITION AND MULTI-RWARD POLICY OPTIMIZATION

Anonymous authors

Paper under double-blind review

## ABSTRACT

Vision-Language Models (VLMs) often suffer from visual hallucinations – generating things that are not consistent with visual inputs – and language shortcuts, where they skip the visual part and just rely on text priors. These issues arise because most post-training methods for VLMs rely on simple verifiable answer matching and supervise only final outputs, leaving intermediate visual reasoning without explicit guidance. As a result, VLMs receive sparse visual signals and often learn to prioritize language-based reasoning over visual perception. To mitigate this, some existing methods add visual supervision using human annotations or distilled labels from external large models. However, human annotations are labor-intensive and costly, and because external signals cannot adapt to the evolving policy, they cause distributional shifts that can lead to reward hacking.

In this paper, we introduce Vision-SR1, a self-rewarding reinforcement learning method that improves visual reasoning without relying on external visual supervisions. Vision-SR1 decomposes VLM reasoning into two stages: *visual perception* and *language reasoning*. The model is first prompted to produce self-contained visual perceptions that are sufficient to answer the question without referring back the input image. To validate this self-containment, the same VLM model is then re-prompted to perform language reasoning using only the generated perception as input to compute reward. This self-reward is combined with supervision on the final outputs through multi-reward policy optimization, providing a balanced training signal that strengthens both visual perception and language reasoning. In addition, Multi-Reward Policy Optimization separately computes advantages and log probabilities for both the visual reasoning reward and the answer accuracy reward. The method then calculates KL divergence regularization and actor loss using the combined sum of these two reward components. Our experiments show that Vision-SR1 improves visual reasoning, mitigates visual hallucinations, and reduces reliance on language shortcuts across diverse vision-language tasks.

## 1 INTRODUCTION

Recent advances in vision-language models (VLMs) have progressed by integrating pre-trained language models and vision encoders with instruction tuning (Liu et al., 2023b; et al., 2024; Chen et al., 2024; Bai et al., 2025; Li et al., 2025d). Despite these successes, a critical limitation remains in their reasoning capabilities: VLMs often produce visual hallucinations – descriptions of content that is not actually present in the image (Guan et al., 2024; Liu et al., 2024; Li et al., 2025e; Liu et al., 2023a) – or rely on language shortcuts, where the model bypasses visual understanding and instead depends solely on text priors (Si et al., 2022; Bleeker et al., 2024). Very recently, R1-style reinforcement learning (RL) methods have been shown to improve the reasoning abilities of VLMs across diverse tasks (Huang et al., 2025b; Shen et al., 2025; Xia et al., 2025; Zhang et al., 2025). However, these methods often encourage “thinking over seeing” that lean heavily on language reasoning while underutilize visual perception (Liu et al., 2025; Yao et al., 2025). This imbalance makes VLMs susceptible to reward hacking (Fu et al., 2025) and spurious effects (Shao et al., 2025) observed in RL training. Although VLMs trained with RL often have apparent improvements, they can largely re-

054 reflect probability shifts toward the style of training and test data, leading to language shortcut answers  
 055 from prior knowledge and overlooking hallucination risks (Li et al., 2025b).  
 056

057 In essence, most existing post-training methods for VLMs rely on simple verifiable answer matching  
 058 and thus lack explicit supervision of visual information. As a result, VLMs receive sparse visual  
 059 signals and often learn to prioritize language-based reasoning over visual perception. To mitigate  
 060 this, some methods introduce intermediate visual supervision through human annotations (Thawakar  
 061 et al., 2025) or distilled labels (e.g., pre-extracted key steps) from external models (Xu et al., 2024;  
 062 Zhang et al., 2025; Xiao et al., 2025; Xia et al., 2025; Lu et al., 2025). However, these solutions  
 063 face significant limitations. Human annotations are labor-intensive, costly, and difficult to scale  
 064 across multimodal tasks, while distilled signals inherit biases from source models and often fail  
 065 to generalize across diverse domains. Moreover, distributional shifts between fixed intermediate  
 066 signals and the continually updated policy can lead to reward hacking (Gao et al., 2023). Most  
 067 importantly, both approaches remain limited by their reliance on external supervision and their use of  
 068 single advantage and log probability computations across multiple intermediate rewards, , restricting  
 069 their scalability and applicability.

070 In this paper, we introduce **Vision-SR1**, a reinforcement learning framework that encourages VLM  
 071 to produce *self-contained* visual reasoning that can be verified by the VLM itself, without external  
 072 supervision. Vision-SR1 decomposes the reasoning process into two stages: *visual perception* and  
 073 *language reasoning*. The visual perception is required to capture all details relevant to answering  
 074 the query, so that the reasoning stage can proceed without re-accessing the original image. We  
 075 explicitly compute advantages and rollouts separately for each stage, then calculate individual Actor  
 076 policy losses and KL divergence terms for the visual perception and language reasoning stages  
 077 before combining them into a unified training objective.

078 The training has two **rollout passes** and one **training objective optimization** of the same VLM:

079 **– First pass (standard rollout):** (Image, Query) → (Visual Perception, CoT Reasoning, Answer)

- 080 • The model generates a structured output that explicitly separates visual perception, chain-  
 081 of-thought (CoT) reasoning, and the final answer.
- 082 • An **accuracy reward** is computed by comparing the final answer with the ground truth.

083 **– Second pass (self-reward rollout):** (Query, Visual Perception) → (CoT Reasoning, Answer)

- 084 • The model is re-prompted to reason using only the generated perception (without re-  
 085 accessing the original image). If the correct answer is derived, the perception is considered  
 086 **faithful**, and a **self-visual reward** is assigned.

087 **– Multi-Reward Policy Optimization (objective optimization):**

- 088 • The multi-reward policy optimization enables the policy model to receive distinct feedback  
 089 for visual reasoning quality and answer accuracy through separate advantage computations  
 090 and rollout-specific loss terms.

091 These separate reward signals are then combined through our multi-policy loss objective to pro-  
 092 vide balanced training that strengthens both visual perception and language reasoning without the  
 093 entangled learning signals of traditional reward summation. Experiments show that Vision-SR1  
 094 improves visual reasoning, mitigates hallucinations, and reduces language shortcuts across diverse  
 095 vision-language tasks.

## 096 2 METHOD

100 We build upon advancement of Group Relative Policy Optimization (GRPO) (Shao et al., 2024) for  
 101 improving VLM reasoning. We first review the key concepts then introduce our method.  
 102

### 103 2.1 PRELIMINARY: REINFORCEMENT LEARNING FOR VLM WITH VERIFIABLE REWARD

104 We denote a pre-trained VLM as a policy model  $\pi$  to be optimized in reinforcement learning. Given  
 105 a multimodal question ( $Q$ ) consists of an image  $i$  and a text question  $q$ , where  $Q = \{i, q\}$ , the policy  
 106 model  $\pi$  generates a reasoning response  $s$ . We use GRPO to optimize the response  $s$  for the policy  
 107 model. For each multimodal question  $Q = \{i, q\}$  we sample a *group* of  $K$  candidate responses

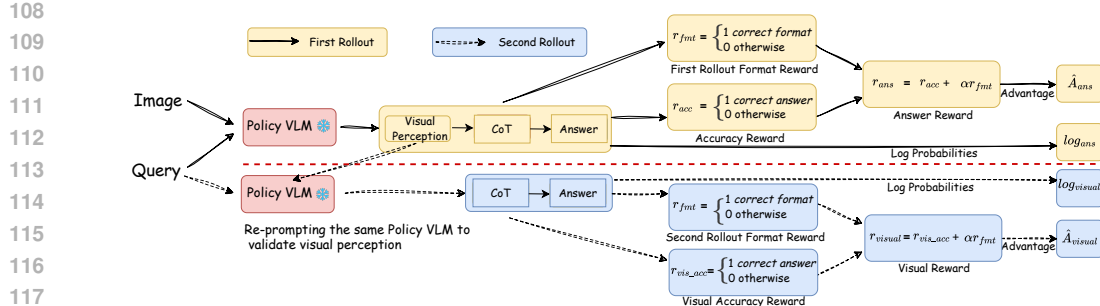


Figure 1: Overall framework of Vision-SR1. During RL training, the VLM performs two rollouts. In the first pass, the model takes an image–query pair and generates a structured output (visual perception, CoT reasoning, and answer), with answer reward computed against the ground truth. In the second pass, the model is re-prompted to answer using only query and its generated visual perception. If the correct answer is derived, a self-visual reward is assigned. We compute the advantages and log probabilities for each rollout for Multi-Reward Policy Optimization.

$S_Q = \{s_1, \dots, s_K\}$ ,  $s_k \sim \pi_\theta(\cdot | Q)$ . Each response is scored by a scalar reward  $r(Q, s_k)$  (defined in Sec. 2.2), and we compute a *group-relative* advantage

$$\hat{A}^{\text{grp}}(Q, s_k) = r(Q, s_k) - \frac{1}{K} \sum_{j=1}^K r(Q, s_j), \quad (1)$$

which centres rewards within the group, removing question-level biases while retaining pairwise preferences. We update the policy by maximizing

$$\mathcal{L}_{\text{GRPO}}(\theta) = \mathbb{E}_{Q \sim \mathcal{D}} \left[ \sum_{k=1}^K \hat{A}^{\text{grp}}(Q, s_k) \log \pi_\theta(s_k | Q) - \beta \text{KL}(\pi_\theta(\cdot | Q) \| \pi_{\theta_0}(\cdot | Q)) \right], \quad (2)$$

where  $\pi_{\theta_0}$  is the frozen, pre-trained reference model and  $\beta$  controls the strength of the KL penalty that keeps the updated policy close to its original behavior.

The group-centred baseline in equation 1 guarantees  $\sum_k \hat{A}^{\text{grp}}(Q, s_k) = 0$ , thereby reducing the variance of policy-gradient estimates without requiring an external value critic.

## 2.2 STEPS 1: SELF-REWARDING VLM VIA REASONING DECOMPOSITION

As we discussed, incorporating intermediate visual supervision can strengthen the reasoning ability of VLMs. However, existing methods suffer from key limitations: methods based on human annotations are labor-intensive and costly (Thawakar et al., 2025), while approaches that distill supervision from external models provide static signals that cannot adapt as the policy model itself evolves during training (Zhang et al., 2025; Xiao et al., 2025; Xia et al., 2025). To overcome these issues, we introduce a self-rewarding framework that enables the VLM to reward its own visual perception. The key idea is to decompose the visual reasoning process into structured components, i.e., the VLM first produces a self-contained visual perception and then assesses whether this perception is sufficient for produce the final answer. This decomposition reduces reliance on external supervision and allows the reward signal to adapt dynamically as the model improves.

**Decomposed VLM Reasoning.** To encourage the VLM to perform self-contained visual reasoning, we require every response to adhere to a *See-Think* generation format (Jia et al., 2024; Xia et al., 2025) format. Specifically, for a vision-language task,  $Q = \{i, q\}$  where  $i$  is the input image and  $q$  is the textual query, the model produces the following structured output:

$\langle \text{visual\_reasoning} \rangle c \langle / \text{visual\_reasoning} \rangle \| \langle \text{think} \rangle t \langle / \text{think} \rangle \| \langle \text{answer} \rangle a \langle / \text{answer} \rangle$

where  $c$  is a *self-contained* visual perception that captures all visual information necessary to solve the task, so that the following language reasoning can proceed without re-accessing the original input image. Besides,  $t$  is the language reasoning trace, and  $a$  denotes the final answer.

162 **Self-Reward for Visual Reasoning.** A challenge is judging whether the visual perception  $c$  is  
 163 *self-contained* – i.e. whether it encodes *all* the visual information needed to answer the question  
 164  $Q = \{i, q\}$  correctly. To address this, our idea is to treat the visual perception as a *text-only proxy*  
 165 for the image and validate it by re-prompting the VLM itself to perform language reasoning using  
 166 only the generated perception as input. If the model can derive the correct answer from  $(c, q)$  alone,  
 167 we consider  $c$  to be visually faithful and assign the corresponding visual reward.

$$\hat{a} = f_\theta(c, q), \quad r_{\text{visual}}(Q, c) = \mathbb{I}[\hat{a} = a^*], \quad (3)$$

170 where  $a^*$  is the ground-truth answer. Instead of using an external reward model, we leverage the  
 171 policy model’s own reasoning ability for self-evaluation. The model itself determines the reward by  
 172 answering the question using only its generated visual reasoning (Figure 1).  
 173

174 **Reward Composition.** The reward composition comprises three *aligned* components, each con-  
 175 ditioned on the question  $Q = \{i, q\}$ :

176 • **Format reward**  $r_{\text{fmt}}(s)$ : measures whether the response strictly follows the required layout. This  
 177 reward is being applied to both Visual reward and Accuracy reward with respect to their format  
 178 requirements.

179 • **Answer reward**  $r_{\text{ans}}(Q, a)$ : measures the correctness of the final answer ( $r_{\text{acc}}$ ) *plus* the corre-  
 180 sponding format reward. Because  $a$  is generated after the reasoning trace  $t$ , the term implicitly  
 181 rewards CoT reasoning. This is computed at first rollout with hyper-parameters ( $0 \leq \alpha \leq 1$ ):  
 182

$$r_{\text{ans}}(Q, a) = r_{\text{acc}}(Q, a), +\alpha r_{\text{fmt}}(s) \quad (4)$$

184 • **Visual reward**  $r_{\text{visual}}(Q, c)$ : measures whether the visual reasoning output is self-contained, i.e.,  
 185 sufficient to answer the question without image ( $r_{\text{vis\_acc}}$ ) *plus* corresponding format reward. A  
 186 reward of 1 is assigned if, given only the question and the visual reasoning, the VLM can give the  
 187 correct answer. This is computed at second rollout:  
 188

$$r_{\text{visual}}(Q, c) = r_{\text{vis\_acc}}(Q, c), +\alpha r_{\text{fmt}}(s) \quad (5)$$

### 191 2.3 STEP 2: MULTI-REWARD OPTIMIZATION WITH MULTI-ADVANTAGE LOSS 192 COMPUTATION.

193 Simply *summing* the visual reasoning reward and the final-answer accuracy reward could produce a  
 194 *sparse and entangled* learning signal: the policy has little to tell which rollout was responsible for  
 195 which part of the scalar return. To disentangle visual reasoning and answer accuracy assignment,  
 196 we keep the two rollouts—answer generation and visual reasoning—*separate* throughout the up-  
 197 date. Each rollout receives its own log-probabilities, advantage, and KL term, and the gradients are  
 198 combined only at the very end. This turns the single *multi-reward* problem into two single-reward  
 199 sub-problems that share parameters with individually optimized feedback.  
 200

201 **Reward-Specific Log-Probability Tracking.** During sampling we cache the behavioral log prob-  
 202 abilities for every token in each rollout:

$$\log \pi_{\text{old}}^{(i)}(a_{\text{ans}, t}), \log \pi_{\text{old}}^{(i)}(a_{\text{visual}, t}),$$

205 where  $a_{\text{ans}, t}$  is the action at step  $t$  of the first rollout, and  $a_{\text{visual}, t}$  is the action (token) at step  $t$  of the  
 206 second rollout. At update time we compute the corresponding  $\log \pi_\theta$  under the current parameters  
 207 to compute the policy and KL losses.

208 **Group-wise Z-Score Advantage.** For each reward we follow GRPO to compute the advantage:  
 209

$$A_{\text{ans}}^{(i)} = \frac{r_{\text{ans}}^{(i)} - \mu_{\text{ans}}}{\sigma_{\text{ans}} + \varepsilon}, \quad A_{\text{visual}}^{(i)} = \frac{r_{\text{visual}}^{(i)} - \mu_{\text{visual}}}{\sigma_{\text{visual}} + \varepsilon}, \quad (6)$$

210 with means and standard deviations  $\mu_{\text{ans}} = \frac{1}{B} \sum_i r_{\text{ans}}^{(i)}$ ,  $\sigma_{\text{ans}}^2 = \frac{1}{B} \sum_i (r_{\text{ans}}^{(i)} - \mu_{\text{ans}})^2$ , where  $B$   
 211 is the rollout batch size (and analogously for the visual group). Broadcasting  $A_{\text{ans}}$  to all caption  
 212 tokens and  $A_{\text{visual}}$  to all answer tokens gives two advantage masks that weight the corresponding  
 213 log-probabilities during backpropagation for each sub-task.

216 **Actor Loss (Policy Gradient Loss).** The actor loss computes weighted policy gradients for the  
 217 two reward signals (answer and visual), with separate coefficients  $\lambda_{\text{ans}}$  and  $\lambda_{\text{visual}}$  indicating their  
 218 contributions.<sup>1</sup>

$$\mathcal{L}_{\text{actor}} = -\frac{\lambda_{\text{ans}}}{B} \sum_{i,t} A_{\text{ans},t}^{(i)} \log \pi_{\theta}(a_{\text{ans},t}^{(i)}) - \frac{\lambda_{\text{visual}}}{B} \sum_{i,t} A_{\text{visual},t}^{(i)} \log \pi_{\theta}(a_{\text{visual},t}^{(i)}) \quad (7)$$

222 **KL Divergence Regularization Loss.** The KL regularization applies separate penalty co-  
 223 efficients  $\beta_{\text{cap}}$  and  $\beta_{\text{ans}}$  to prevent excessive policy deviation for each reward component.  
 224

$$\mathcal{L}_{\text{KL}} = \frac{\beta_{\text{ans}}}{B} \sum_{i=1}^B \sum_t [\log \pi_{\text{old}}(a_{\text{ans},t}^{(i)}) - \log \pi_{\theta}(a_{\text{ans},t}^{(i)})] + \frac{\beta_{\text{visual}}}{B} \sum_{i=1}^B \sum_t [\log \pi_{\text{old}}(a_{\text{visual},t}^{(i)}) - \log \pi_{\theta}(a_{\text{visual},t}^{(i)})] \quad (8)$$

229 **Multi-Reward Loss Objective.** The total loss combines multi-reward policy gradients with  
 230 component-specific regularization to optimize the model across both reward signals.

$$\mathcal{L}_{\text{total}} = \mathcal{L}_{\text{actor}} + \mathcal{L}_{\text{KL}} \quad (9)$$

#### 233 2.4 THEORETICAL ANALYSIS

235 We analyze why Multi-Reward Policy Optimization with separate advantage computation could  
 236 improve VLM RL training compared to using only answer rewards. In standard RL training, the  
 237 objective depends solely on final answer correctness:

$$\nabla_{\theta} \mathbb{E}_{s \sim \pi_{\theta}} [r_{\text{ans}}(a, a^*)] \quad (10)$$

239 where  $s = (t, a)$  contains visual reasoning and language reasoning trace  $t$  and final answer  $a$ . Since  
 240  $r_{\text{ans}}$  only measures whether  $a$  matches ground truth  $a^*$ , the intermediate visual reasoning  $t$  receives  
 241 no direct supervision signal. For VLMs, the stronger LLM backbone dominates generation of  $t$ , and  
 242 continued RL training leads to potential reward hacking where the model exploits language priors  
 243 to achieve correct answers without visual grounding [Pantazopoulos & Özyigit \(2025\)](#).

244 **Multi-Reward Loss Decomposition.** We decompose the loss computation itself into separate com-  
 245 ponents as shown in Equation 9, where the actor loss handles visual and answer components sepa-  
 246 rately (with the  $KL$  regularization term following similar component-wise structure):

$$\mathcal{L}_{\text{actor}} = -\lambda_{\text{ans}} \mathbb{E}[A_{\text{ans}} \log \pi_{\theta}(a_{\text{ans}})] - \lambda_{\text{visual}} \mathbb{E}[A_{\text{visual}} \log \pi_{\theta}(a_{\text{visual}})] \quad (11)$$

248 Since each advantage is computed from different reward components (visual and answer) shown  
 249 in Equation 6, this approach creates clear gradient paths from each reward to its corresponding  
 250 components, enabling independent optimization of visual reasoning and language reasoning capa-  
 251 bilities [\(Zhu et al., 2025; Lyu et al., 2025\)](#).

253 From an information-theoretic perspective, let  $I$  denote the visual input,  $Q$  the question,  $C$  the  
 254 visual reasoning representation, and  $A$  the final answer. Mutual information  $I(U; V)$  measures how  
 255 much knowing  $U$  reduces uncertainty about  $V$  [\(Shannon, 1948\)](#). If training relies only on  $r_{\text{ans}}$ , the  
 256 model primarily maximizes  $I(A; Q)$ —making answers strongly dependent on the question—while  
 257 neglecting  $I(A; I)$ , the dependence of answers on the visual input. This permits shortcut solutions  
 258 that bypass perception. By additionally optimizing  $r_{\text{visual}}$ , which enforces high  $I(C; I)$ , the model  
 259 strengthens the path from  $I$  to  $A$ , thereby increasing  $I(A; I)$  and ensuring that answers remain  
 260 grounded in visual reasoning rather than language-only correlations.

#### 261 2.5 DATA PREPARATION

263 **Vision-SR1-47K.** Our RL dataset consists of approximately 47K examples collected from 24 open-  
 264 source VLM benchmarks. It spans three key reasoning domains (Figure 1): mathematical reasoning  
 265 (30.5%), which strengthens quantitative and logical abilities; commonsense knowledge (30%); and  
 266 general visual understanding (39.5%), which grounds the model in visual question answering.

## 268 3 EXPERIMENTS

269 <sup>1</sup>We use 0.5 for  $\lambda_{\text{ans}}$  and  $\lambda_{\text{visual}}$ .

To implement our Vision-SR1, we use **Qwen2.5-VL-3B** and **7B**, Mimo-7B-VL **Team et al. (2025)** as base models. Additionally, we use Lora finetuning to train Qwen2.5-VL-72B to evaluate the method’s generalization to larger model sizes and Lora finetuning.<sup>2</sup> We train the base model with GRPO. The RL phase is trained for 1 epoch on the Vision-SR1-47K dataset. During training, the policy model first generates visual reasoning from the input image, then produces language reasoning and final answer. We then compute a self-reward for visual reasoning by re-prompting the frozen policy model to answer the question using only its generated visual reasoning, without access to the original image  $i$ . Finally, we compute advantages and log probabilities separately for each reward component and combine them in the final loss (Figure 1).<sup>3</sup>

Table 1: Vision-SR1-47K data comprises three domains—Math, Knowledge, and General Visual Reasoning—providing diverse supervision for VLM generalization and adaptation.

Category	Included Datasets	Size	(%)
Math	CLEVR-Math, GeoQA+, UniGeo, GEOS, Geometry3K, Super-CLEVR	14K	30.5%
Science Knowledge	TQA, ScienceQA, A12D, PMC-VQA, VQA-RAD, EXAMS-V-train	14K	30%
General Visual Reasoning	ChartQA, DVQA, PlotQA, FigureQA, MapQA, TabMWP, A-OKVQA, IconQA, visual7w, OpenSpaces, Spacellava	18K	39.5%

### 3.1 BASELINE METHODS

**Vision-R1** (**Huang et al., 2025b**): The first R1-style reinforcement learning approach, which relies solely on answer rewards as the training signal. However, since the original Vision-R1 was trained only on math-domain data and performs poorly on general-domain reasoning, we reproduce it using our 47K dataset to ensure a fair comparison.

**Perception-R1** (**Xiao et al., 2025**): Similar in training style to Vision-R1, but incorporates pre-extracted visual annotations as an additional reward signal. These visual annotations are derived from a state-of-the-art proprietary multimodal LLM (not specified in the paper).

**Visionary-R1** (**Xia et al., 2025**): Trained to produce a caption–reason–answer output format during RL, where the supervision signal comes from an external text-only LLM (not specified in the paper).

For fair comparisons, we only re-train Vision-R1 on our 47K dataset, since both Perception-R1 and Visionary-R1 require access to external annotations or supervision signals, which are undisclosed.

### 3.2 BENCHMARKS AND METRICS

Our evaluation covers three areas to evaluate VLMs abilities. Specifically, the domains include (1) general visual understanding, (2) multimodal math reasoning (3) visual hallucination detection.

**General Visual Understanding.** We evaluate general visual understanding across five diverse benchmarks. **MMMU** (**Yue et al., 2024**) tests cross-modal reasoning and subject knowledge with 11.5K college-level, four-choice questions spanning six disciplines. **MMMU-Pro** (**Yue et al., 2025**) increases the difficulty with ten choices per question and adds a challenging *vision-only* setting, where all text is embedded within the image to necessitate robust visual parsing. **Real-WorldQA** (**xAI, 2024**) features ~700 real-world images from vehicle captures, paired with spatially grounded questions that require verifiable answers. **VisNumBench** (**Weng et al., 2025**) specifically targets visual number sense through ~1.9K questions covering seven numerical attributes and four estimation tasks.

**Multimodal Mathematical Reasoning.** We assess mathematical reasoning using two specialized benchmarks. **MathVerse** (**Zhang et al., 2024a**) consists of 2.6K diagram-centric problems (e.g., geometry, functions), each rendered in six visual-text variants to disentangle true visual understanding from linguistic shortcuts. Evaluation is based on step-by-step Chain-of-Thought (CoT) correctness. **MATH-Vision** (**Wang et al., 2024**) presents ~3K competition-grade problems across 16 disciplines and five difficulty levels, stressing advanced multimodal reasoning.

<sup>2</sup>For Qwen2.5-VL-72B, we used ms-swift **Zhao et al. (2024)** to perform Lora finetuning on 80 steps, batch size 8 for resource and time limitation. For 72B finetuning, the Lora adapter is frozen during both rollouts.

<sup>3</sup>The policy model remains frozen during both rollouts.

324 Table 2: Vision-SR1 vs. baselines. For Vision-R1, as noted in Section 3.1, the original model  
 325 checkpoint was trained only on math-domain data. So we also reproduce it using our 47K dataset.

327 Methods	328 General Visual Understanding				329 Visual Math & Hallucination			330 Avg.
	331 MMMU -Pro	332 MMMU	333 RealWorld QA	334 VisNum Bench	335 Math Verse	336 MATH -Vision	337 Hallusion Bench	
Visionary-R1 (3B) by <a href="#">Xia et al. (2025)</a>	27.4	30.6	56.9	10.0	45.0	40.4	26.7	33.9
Perception-R1 (7B) by <a href="#">Xiao et al. (2025)</a>	36.8	40.9	69.4	15.9	52.1	35.7	65.4	45.2
Vision-R1 (7B) by <a href="#">Huang et al. (2025b)</a>	34.9	42.8	60.1	33.0	57.3	51.2	32.2	44.5
<i>Backbone model: Qwen2.5-VL-3B</i>								
Zero-shot Inference (before RL)	30.5	25.5	65.4	15.7	44.3	40.4	27.1	35.5
Vision-R1 47K data (fair comparison)	40.3	49.5	63.0	36.7	42.8	29.9	67.4	47.1
<b>Vision-SR1 (ours)</b>	<b>40.8</b>	<b>49.6</b>	<b>66.1</b>	<b>41.9</b>	<b>45.8</b>	<b>29.3</b>	<b>68.3</b>	<b>48.8</b>
<i>Backbone model: Qwen2.5-VL-7B</i>								
Zero-shot Inference (before RL)	34.2	33.5	68.5	21.4	49.2	31.9	51.7	41.5
Vision-R1 47K data (fair comparison)	39.8	51.8	66.6	43	53.2	33.8	66.6	50.7
<b>Vision-SR1 (ours)</b>	<b>40.7</b>	<b>52.2</b>	<b>69.2</b>	<b>43.5</b>	<b>54.5</b>	<b>36.2</b>	<b>68.9</b>	<b>52.2</b>
<i>Backbone model: Mimo-VL-7B</i>								
Zero-shot Inference (before RL)	38.0	45.6	68.2	30.2	35.5	21.6	71.9	44.4
Vision-R1 47K data (fair comparison)	38.7	47.3	67.1	33.5	35.3	25.7	74.3	46.0
<b>Vision-SR1 (ours)</b>	<b>39.3</b>	<b>49.5</b>	<b>68.1</b>	<b>44.6</b>	<b>40.0</b>	<b>29.6</b>	<b>75.6</b>	<b>49.5</b>
<i>Backbone model: Qwen2.5-VL-72B</i>								
Zero-shot Inference (before Lora RL)	40.6	45.0	69.5	26.1	51.3	33.5	68.7	47.8
Vision-R1 47K data (fair comparison)	43.8	45.3	72.1	47.1	50.5	34.6	73.2	52.4
<b>Vision-SR1 (ours)</b>	<b>47.6</b>	<b>52.8</b>	<b>75.1</b>	<b>47.9</b>	<b>53.6</b>	<b>34.5</b>	<b>74.4</b>	<b>55.1</b>

342  
 343 **Hallucination Diagnosis.** To diagnose model failures, we use **HallusionBench** ([Guan et al., 2024](#)),  
 344 a benchmark designed to pinpoint specific errors: (i) language-side hallucination, where visual con-  
 345 text is ignored, and (ii) visual-illusion errors, where the image is misinterpreted. The benchmark’s  
 346 binary yes/no format enables precise error analysis.

347 For our evaluations, we all use Gemini-2.5-flash ([Comanici et al., 2025](#)) to judge response correct-  
 348 ness on non-multiple choice format question, serving as a proxy for human judgment.

### 350 3.3 EXPERIMENTAL RESULTS

#### 352 3.3.1 VISION-SR1 V.S. BASELINE METHODS

354 Table 2 presents a comprehensive comparison  
 355 of Vision-SR1 with several baseline methods  
 356 across diverse vision-language benchmarks.  
 357 For example, with the Qwen2.5VL-72B back-  
 358 bone, Vision-SR1 reaches 47.6 on MMMU-Pro  
 359 and 52.8 on MMMU, outperforming Vision-  
 360 R1 fair comparison runs (43.8 and 45.3, re-  
 361 spectively). When averaged across all bench-  
 362 marks, Vision-SR1 establishes a clear margin  
 363 of improvement. With the 72B backbone, it  
 364 achieves an average score of 55.1, compared  
 365 to 52.4 for Vision-R1. Even with the smaller  
 366 3B and 7B backbone, Vision-SR1 achieve 48.8  
 367 and 52.2 average, outperforming all compara-  
 368 ble baselines. For results on Mimi-VL-7B, a  
 369 model outside the Qwen-VL family, we observe a similar trend: the average accuracy improves  
 370 from 44.4 to 49.5. This shows that our method generalizes beyond the Qwen-VL. These results  
 371 demonstrate that Vision-SR1 outperforms prior baseline models across both general-purpose and  
 372 math-specific visual reasoning tasks, validating the effectiveness of our approach.

#### 373 3.3.2 ABLATION STUDY ON SPATIAL REASONING AND LANGUAGE SHORTCUT DATASETS

374 In addition to evaluating Vision-SR1 on standard visual-reasoning benchmarks, we further evaluate  
 375 its effectiveness on additional datasets to probe two complementary challenges: spatial reasoning  
 376 and language-shortcut (LS) robustness. MMSI-Bench [Yang et al. \(2025\)](#) and OmniSpatial [Jia et al.](#)  
 377 ([2025](#)) target multi-image spatial understanding, requiring models to integrate spatial relationships  
 across multiple images. In contrast, ViLP [Luo et al. \(2025\)](#) evaluates language shortcuts by pairing

378 Table 3: Our method also can improve VLMs’  
 379 abilities on spatial reasoning and language short-  
 380 cut (LS) robustness.

381 Methods	382 ViLP (LS)	383 MMSI -Bench	384 Omni Spatial	385 Avg.
<i>Backbone: Mimo-VL-7B</i>				
before RL	56.4	28.2	40.3	41.6
Vision-R1	58.2	27.7	40.4	42.1
<b>Vision-SR1</b>	<b>59.3</b>	<b>28.0</b>	<b>42.7</b>	<b>43.3</b>
<i>Backbone: Qwen2.5-VL-7B</i>				
before RL	45.1	24.0	27.3	32.1
Vision-R1	51.3	21.9	31.1	34.8
<b>Vision-SR1</b>	<b>52.6</b>	<b>27.7</b>	<b>44.2</b>	<b>41.5</b>
<i>Backbone: Qwen2.5-VL-72B</i>				
Zero-shot	55.9	33.4	36.5	41.9
Vision-R1 (Lora)	55.4	35.4	36.4	42.4
<b>Vision-SR1 (Lora)</b>	<b>61.8</b>	<b>35.3</b>	<b>38.6</b>	<b>45.2</b>

each question with images that can be answered either through textual priors alone or only through pure visual reasoning. Table 3 shows that Vision-SR1 generalizes well to spatial reasoning benchmarks and substantially improves robustness to visual–language shortcuts. In particular, explicitly generating visual descriptions helps the model avoid shortcut behavior and rely more on the actual visual content. Next we propose a systematic way to evaluate VLMs’ language shortcut frequencies on standard VLM benchmarks.

### 3.3.3 ANALYSIS ON LANGUAGE SHORTCUT

Table 4: Language Shortcut Rate (LSR) across different benchmarks. Lower values indicate better performance, as a reduced LSR reflects fewer language shortcuts during reasoning. Adding additional reward supervision can reduce the chance of visual reasoning reward hacking.

Methods	General Visual Understanding				Visual Math & Hallucination			
	MMMU -Pro	MMMU	RealWorld QA	VisNum Bench	Math Verse	MATH -Vision	Hallusion Bench	Avg.
Vision-SR1 (3B)	7.5	6.3	10.8	5.4	10.3	8.3	10.1	9.4
└ w/o self-reward	9.0	9.6	11.9	4.2	11.4	9.2	8.5	10.4
Vision-SR1 (7B)	8.0	6.5	13.4	4.2	11.5	10.7	6.8	9.8
└ w/o self-reward	8.7	5.3	10.8	3.9	12.7	10.7	9.1	10.1

We also introduce the Language Shortcut Rate (LSR), a metric designed to quantify how often a model produces the correct answer with an incorrect visual perception. A high LSR suggests the model is leveraging language knowledge prior rather than genuine visual understanding.

Our evaluation, follows a two-step process and uses Gemini-2.5-flash as a judge: (1) Visual Perception Extraction: for each model output, we extracted the generated visual reasoning, denoted as  $\hat{C}$ . (2) Self-Containment Check: we then provide the  $\hat{C}$  and the original question  $Q$  to Gemini-2.5-Flash evaluator. If the evaluator can reproduce the correct ground-truth answer using *only* this information,  $\hat{C}$  is deemed self-contained. Based on this process, we define the metrics: The **Language Shortcut Rate (LSR)** is defined as the percentage of instances where the model produces an *incorrect (not self-contained) visual reasoning* but still gives the *correct final answer*:

$$\text{LSR} = \frac{\#\{\text{incorrect visual reasoning \& correct answer}\}}{\#\{\text{total samples}\}}$$

A higher LSR indicates that the model is answering correctly while bypassing visual perception, suggesting reliance on language prior shortcuts. An LSR of 0 indicates no shortcircuiting, i.e., every correct answer is supported by a correct, self-contained visual reasoning.

We compute the LSR for 7B model w/ and w/o self rewards on seven selected benchmarks for demo example in Table 4. An important finding is that the visual shortcut is the *highest in multimodal mathematical reasoning*, which raises important question to previous work R1-VL (Zhang et al., 2025), VLM-R1 (Shen et al., 2025), Vision-R1 (Huang et al., 2025b): is multimodal RL training truly improving VLMs’ abilities to perform visual reasoning, or simply awakes the models’ language reasoning ability to guess without actually looking at visual information?

## 4 RELATED WORK

### 4.1 POST-TRAINING VISION-LANGUAGE MODELS

Recent vision-language models have increasingly leveraged post-training alignment techniques, including instruction tuning and reinforcement learning, to enhance general-purpose multimodal performance (Liu et al., 2023b; Bai et al., 2025; Chen et al., 2024; et al, 2024; Huang et al., 2025b). For example, LLaVA (Liu et al., 2023b) is tuned on GPT-4 generated (image, question, answer) pairs, coupling a CLIP encoder with Vicuna to produce a visual chat assistant that imitates some GPT-4 vision capabilities. InstructBLIP (Dai et al., 2023) introduces an instruction-aware query transformer tuned on 26 datasets, which yields a model that substantially outperforms even larger models on zero-shot benchmarks. Beyond standard instruction-tuning methods like LLaVA and Instruct-BLIP, recent work increasingly uses reinforcement learning (RL) to align vision-language models

432 for better reasoning (Huang et al., 2025b; Xia et al., 2025; Xiao et al., 2025). Many of these meth-  
 433 ods, inspired by techniques from DeepSeek-R1 (DeepSeek-AI et al., 2025), focus on sophisticated  
 434 reward engineering. Strategies include providing step-wise rewards to supervise the intermediate  
 435 reasoning (Zhang et al., 2025), adding explicit visual annotations to ground truth for calculating  
 436 visual rewards (Xiao et al., 2025), and applying RL in a two-stage curriculum that first strengthens  
 437 text-only reasoning (Peng et al., 2025b). As a complementary approach, RL from AI Feedback  
 438 for VLMs demonstrates that preference-based alignment is also a powerful signal, showing it can  
 439 substantially reduce object hallucination by learning from AI-generated feedback (Yu et al., 2024).

## 441 4.2 SELF-REWARDING REINFORCEMENT LEARNING

443 The existing reinforcement learning with verifiable rewards (RLVR) methods heavily rely on high-  
 444 quality reward models or human feedback, creating a major bottleneck for scalability (Peng et al.,  
 445 2025a; Dai et al., 2025; Li et al., 2025c; Luu et al., 2025). To overcome this, recent work explores  
 446 self-rewarding approaches, where the model itself provides intrinsic reward signals during RL post-  
 447 training, an idea first pioneered by Yuan et al. (2025). Building on self-rewarding language models,  
 448 methods replace external reward models with the model’s own confidence and uncertainty (logit-  
 449 based self-certainty) or self-verification of its solutions, and even elicit a latent *endogenous* reward  
 450 already present inside base LLMs (Zhao et al., 2025; Li et al., 2025a; Simonds et al., 2025; Zheng  
 451 et al., 2025; van Niekerk et al., 2025; Huang et al., 2025a; Zhou et al., 2025). For example, RLIF  
 452 leverages self-certainty as a reward, achieving comparable performance to GRPO while improving  
 453 out-of-distribution generalization (Zhao et al., 2025). Similarly, RLSC optimizes a self-confidence  
 454 reward to secure large accuracy gains with only a few training samples (Li et al., 2025a).

455 Although self-generated reward signals have thrived in text-only LLMs, only a few works extend  
 456 this idea to VLMs (Zhou et al., 2024; Lee et al., 2025; Holmes & Chi, 2025), largely due to the  
 457 complexity of the visual modality and the difficulty of properly defining and evaluating reward  
 458 signals that capture visual perception. Recent progress includes Calibrated Self-Rewarding, which  
 459 iteratively generates candidates, self-scores them with step-wise, visually constrained rewards, and  
 460 fine-tunes via direct preference optimization (DPO) (Zhou et al., 2024). Similarly, RG-VLM uses  
 461 a VLM to directly label rewards for offline trajectories in long-horizon visual tasks, serving as an  
 462 auxiliary signal that boosts generalization (Lee et al., 2025). Beyond judgment-based signals, ARES  
 463 derives dense shaped rewards from attention weights to accelerate learning under sparse or delayed  
 464 feedback (Holmes & Chi, 2025). These works show that internal visual signals can provide rich  
 465 reward feedback for VLM alignment without costly supervision, yet the reward is not integrated  
 466 end-to-end, where the policy receives both visual perception and answer rewards during training.

## 467 5 CONCLUSION AND FUTURE WORK

469 In this paper, we introduce Vision-SR1, a self-rewarded reinforcement learning framework that de-  
 470 composes vision-language understanding into visual reasoning and language reasoning components.  
 471 Our approach uses the VLM itself to generate explicit rewards for visual understanding, then applies  
 472 Multi-Reward Policy Optimization to provide clear gradient attribution and backpropagation path-  
 473 ways for each reward component. Vision-SR1 strengthens visual perception and reduces language  
 474 shortcuts, thereby improving VLM performance across several domains of vision-language tasks.  
 475 Our proposed metric LSR further shows how perception reward lowers the tendency of models to  
 476 answer via language shortcut rather than genuine visual reasoning.

477 This work opens up several future research directions. First, future work can focus on improving the  
 478 efficiency of the *visual reasoning then think* generation format by treating the visual reasoning com-  
 479 ponent as latent thinking, thereby reducing the number of decoded tokens while still enabling reward  
 480 attribution to latent visual processes during the RL phase. It is also important to recognize that some  
 481 of the observed mathematical gains from RL training in VLMs may come from spurious effects –  
 482 for instance, recalibrating the LLM backbone’s output distribution can boost multimodal math per-  
 483 formance without true visual grounding (Shao et al., 2025). This suggests that improvements in  
 484 accuracy may sometimes reflect better exploitation of language shortcuts rather than genuine per-  
 485 ception gains. Therefore, future work can also explore more analysis to disentangle visual grounding  
 from shortcut learning.

486 REPRODUCIBILITY STATEMENT  
487488 To ensure the reproducibility of our research, we provide information regarding our prompt tem-  
489 plates and experimental setup in the main paper and Appendix. All datasets and code will be released  
490 upon conference decision release.  
491492 REFERENCES  
493494 Shuai Bai, Keqin Chen, Xuejing Liu, Jialin Wang, Wenbin Ge, Sibo Song, Kai Dang, Peng Wang,  
495 Shijie Wang, Jun Tang, Humen Zhong, Yuanzhi Zhu, Mingkun Yang, Zhaohai Li, Jianqiang Wan,  
496 Pengfei Wang, Wei Ding, Zheren Fu, Yiheng Xu, Jiabo Ye, Xi Zhang, Tianbao Xie, Zesen Cheng,  
497 Hang Zhang, Zhibo Yang, Haiyang Xu, and Junyang Lin. Qwen2.5-vl technical report, 2025.  
498 URL <https://arxiv.org/abs/2502.13923>.499 Maurits Bleeker, Mariya Hendriksen, Andrew Yates, and Maarten de Rijke. Demonstrating and  
500 reducing shortcuts in vision-language representation learning, 2024. URL <https://arxiv.org/abs/2402.17510>.  
501503 Zhe Chen, Jiannan Wu, Wenhui Wang, Weijie Su, Guo Chen, Sen Xing, Muyan Zhong, Qinglong  
504 Zhang, Xizhou Zhu, Lewei Lu, et al. Internvl: Scaling up vision foundation models and aligning  
505 for generic visual-linguistic tasks. In *Proceedings of the IEEE/CVF conference on computer  
506 vision and pattern recognition*, pp. 24185–24198, 2024.507 Gheorghe Comanici, Eric Bieber, and et al. Gemini 2.5: Pushing the frontier with advanced  
508 reasoning, multimodality, long context, and next generation agentic capabilities, 2025. URL  
509 <https://arxiv.org/abs/2507.06261>.  
510511 Runpeng Dai, Tong Zheng, Run Yang, and Hongtu Zhu. R1-re: Cross-domain relationship extraction  
512 with rlrv. *arXiv preprint arXiv:2507.04642*, 2025.513 Wenliang Dai, Junnan Li, Dongxu Li, Anthony Meng Huat Tiong, Junqi Zhao, Weisheng Wang,  
514 Boyang Li, Pascale Fung, and Steven Hoi. Instructblip: Towards general-purpose vision-language  
515 models with instruction tuning, 2023. URL <https://arxiv.org/abs/2305.06500>.  
516517 DeepSeek-AI, Daya Guo, Dejian Yang, Haowei Zhang, Junxiao Song, Ruoyu Zhang, Runxin Xu,  
518 Qihao Zhu, Shirong Ma, Peiyi Wang, Xiao Bi, Xiaokang Zhang, Xingkai Yu, Yu Wu, Z. F. Wu,  
519 Zhibin Gou, Zhihong Shao, Zhuoshu Li, Ziyi Gao, Aixin Liu, Bing Xue, Bingxuan Wang, Bochao  
520 Wu, Bei Feng, Chengda Lu, Chenggang Zhao, Chengqi Deng, Chenyu Zhang, Chong Ruan,  
521 Damai Dai, Deli Chen, Dongjie Ji, Erhang Li, Fangyun Lin, Fucong Dai, Fuli Luo, Guangbo Hao,  
522 Guanting Chen, Guowei Li, H. Zhang, Han Bao, Hanwei Xu, Haocheng Wang, Honghui Ding,  
523 Huajian Xin, Huazuo Gao, Hui Qu, Hui Li, Jianzhong Guo, Jiashi Li, Jiawei Wang, Jingchang  
524 Chen, Jingyang Yuan, Junjie Qiu, Junlong Li, J. L. Cai, Jiaqi Ni, Jian Liang, Jin Chen, Kai  
525 Dong, Kai Hu, Kaige Gao, Kang Guan, Kexin Huang, Kuai Yu, Lean Wang, Lecong Zhang,  
526 Liang Zhao, Litong Wang, Liyue Zhang, Lei Xu, Leyi Xia, Mingchuan Zhang, Minghua Zhang,  
527 Minghui Tang, Meng Li, Miaojun Wang, Mingming Li, Ning Tian, Panpan Huang, Peng Zhang,  
528 Qiancheng Wang, Qinyu Chen, Qiushi Du, Ruiqi Ge, Ruisong Zhang, Ruizhe Pan, Runji Wang,  
529 R. J. Chen, R. L. Jin, Ruyi Chen, Shanghao Lu, Shangyan Zhou, Shanhua Chen, Shengfeng  
530 Ye, Shiyu Wang, Shuiping Yu, Shunfeng Zhou, Shuting Pan, S. S. Li, Shuang Zhou, Shaoqing  
531 Wu, Shengfeng Ye, Tao Yun, Tian Pei, Tianyu Sun, T. Wang, Wangding Zeng, Wanjia Zhao, Wen  
532 Liu, Wenfeng Liang, Wenjun Gao, Wenqin Yu, Wentao Zhang, W. L. Xiao, Wei An, Xiaodong  
533 Liu, Xiaohan Wang, Xiaokang Chen, Xiaotao Nie, Xin Cheng, Xin Liu, Xin Xie, Xingchao Liu,  
534 Xinyu Yang, Xinyuan Li, Xuecheng Su, Xuheng Lin, X. Q. Li, Xiangyue Jin, Xiaojin Shen, Xi-  
535 aoshua Chen, Xiaowen Sun, Xiaoxiang Wang, Xinnan Song, Xinyi Zhou, Xianzu Wang, Xinxia  
536 Shan, Y. K. Li, Y. Q. Wang, Y. X. Wei, Yang Zhang, Yanhong Xu, Yao Li, Yao Zhao, Yaofeng  
537 Sun, Yaohui Wang, Yi Yu, Yichao Zhang, Yifan Shi, Yiliang Xiong, Ying He, Yishi Piao, Yisong  
538 Wang, Yixuan Tan, Yiyang Ma, Yiyuan Liu, Yongqiang Guo, Yuan Ou, Yuduan Wang, Yue Gong,  
539 Yuheng Zou, Yujia He, Yunfan Xiong, Yuxiang Luo, Yuxiang You, Yuxuan Liu, Yuyang Zhou,  
Y. X. Zhu, Yanhong Xu, Yanping Huang, Yaohui Li, Yi Zheng, Yuchen Zhu, Yunxian Ma, Ying  
Tang, Yukun Zha, Yuting Yan, Z. Z. Ren, Zehui Ren, Zhangli Sha, Zhe Fu, Zhean Xu, Zhenda  
Xie, Zhengyan Zhang, Zhewen Hao, Zhicheng Ma, Zhigang Yan, Zhiyu Wu, Zihui Gu, Zijia Zhu,

540 Zijun Liu, Zilin Li, Ziwei Xie, Ziyang Song, Zizheng Pan, Zhen Huang, Zhipeng Xu, Zhongyu  
 541 Zhang, and Zhen Zhang. Deepseek-r1: Incentivizing reasoning capability in llms via reinforce-  
 542 ment learning, 2025. URL <https://arxiv.org/abs/2501.12948>.

543

544 OpenAI et al. Gpt-4 technical report, 2024. URL <https://arxiv.org/abs/2303.08774>.

545

546 Jiayi Fu, Xuandong Zhao, Chengyuan Yao, Heng Wang, Qi Han, and Yanghua Xiao. Reward  
 547 shaping to mitigate reward hacking in rlhf, 2025. URL <https://arxiv.org/abs/2502.18770>.

548

549 Leo Gao, John Schulman, and Jacob Hilton. Scaling laws for reward model overoptimization. In  
 550 *International Conference on Machine Learning*, pp. 10835–10866. PMLR, 2023.

551

552 Tianrui Guan, Fuxiao Liu, Xiyang Wu, Ruiqi Xian, Zongxia Li, Xiaoyu Liu, Xijun Wang, Lichang  
 553 Chen, Furong Huang, Yaser Yacoob, Dinesh Manocha, and Tianyi Zhou. Hallusionbench: An  
 554 advanced diagnostic suite for entangled language hallucination and visual illusion in large vision-  
 555 language models. In *Proceedings of the IEEE/CVF Conference on Computer Vision and Pattern  
 556 Recognition (CVPR)*, pp. 14375–14385, June 2024.

557

558 Ian Holmes and Min Chi. Attention-based reward shaping for sparse and delayed rewards, 2025.  
 559 URL <https://arxiv.org/abs/2505.10802>.

560

561 Chengsong Huang, Wenhao Yu, Xiaoyang Wang, Hongming Zhang, Zongxia Li, Ruosen Li, Jiaxin  
 562 Huang, Haitao Mi, and Dong Yu. R-zero: Self-evolving reasoning llm from zero data. 2025a.  
 563 URL <https://arxiv.org/abs/2508.05004>.

564

565 Wenxuan Huang, Bohan Jia, Zijie Zhai, Shaosheng Cao, Zheyu Ye, Fei Zhao, Zhe Xu, Yao Hu, and  
 566 Shaohui Lin. Vision-r1: Incentivizing reasoning capability in multimodal large language models,  
 567 2025b. URL <https://arxiv.org/abs/2503.06749>.

568

569 Mengdi Jia, Zekun Qi, Shaochen Zhang, Wenyao Zhang, Xinqiang Yu, Jiawei He, He Wang, and  
 570 Li Yi. Omnispatial: Towards comprehensive spatial reasoning benchmark for vision language  
 571 models, 2025. URL <https://arxiv.org/abs/2506.03135>.

572

573 Mengzhao Jia, Zhihan Zhang, Wenhao Yu, Fangkai Jiao, and Meng Jiang. Describe-then-reason:  
 574 Improving multimodal mathematical reasoning through visual comprehension training, 2024.  
 575 URL <https://arxiv.org/abs/2404.14604>.

576

577 Younghwan Lee, Tung M. Luu, Donghoon Lee, and Chang D. Yoo. Reward generation via large  
 578 vision-language model in offline reinforcement learning, 2025. URL <https://arxiv.org/abs/2504.08772>.

579

580 Pengyi Li, Matvey Skripkin, Alexander Zubrey, Andrey Kuznetsov, and Ivan Oseledets. Confidence  
 581 is all you need: Few-shot rl fine-tuning of language models, 2025a. URL <https://arxiv.org/abs/2506.06395>.

582

583 Zhimin Li, Haichao Miao, Xinyuan Yan, Valerio Pascucci, Matthew Berger, and Shusen Liu. See  
 584 or recall: A sanity check for the role of vision in solving visualization question answer tasks with  
 585 multimodal llms, 2025b. URL <https://arxiv.org/abs/2504.09809>.

586

587 Zongxia Li, Yapei Chang, Yuhang Zhou, Xiyang Wu, Zichao Liang, Yoo Yeon Sung, and Jordan Lee  
 588 Boyd-Graber. Semantically-aware rewards for open-ended r1 training in free-form generation,  
 589 2025c. URL <https://arxiv.org/abs/2506.15068>.

590

591 Zongxia Li, Xiyang Wu, Hongyang Du, Fuxiao Liu, Huy Nghiem, and Guangyao Shi. A survey  
 592 of state of the art large vision language models: Benchmark evaluations and challenges. In *Pro-  
 593 ceedings of the Computer Vision and Pattern Recognition Conference (CVPR) Workshops*, pp.  
 594 1587–1606, June 2025d.

595

596 Zongxia Li, Xiyang Wu, Guangyao Shi, Yubin Qin, Hongyang Du, Tianyi Zhou, Dinesh Manocha,  
 597 and Jordan Lee Boyd-Graber. Videohallu: Evaluating and mitigating multi-modal hallucinations  
 598 on synthetic video understanding, 2025e. URL <https://arxiv.org/abs/2505.01481>.

594 Chengzhi Liu, Zhongxing Xu, Qingyue Wei, Juncheng Wu, James Zou, Xin Eric Wang, Yuyin Zhou,  
 595 and Sheng Liu. More thinking, less seeing? assessing amplified hallucination in multimodal  
 596 reasoning models, 2025. URL <https://arxiv.org/abs/2505.21523>.

597 Fuxiao Liu, Kevin Lin, Linjie Li, Jianfeng Wang, Yaser Yacoob, and Lijuan Wang. Mitigat-  
 598 ing hallucination in large multi-modal models via robust instruction tuning. *arXiv preprint*  
 600 *arXiv:2306.14565*, 2023a.

601 Hanchao Liu, Wenyuan Xue, Yifei Chen, Dapeng Chen, Xiutian Zhao, Ke Wang, Liping Hou,  
 602 Rongjun Li, and Wei Peng. A survey on hallucination in large vision-language models, 2024.  
 603 URL <https://arxiv.org/abs/2402.00253>.

604 Haotian Liu, Chunyuan Li, Qingsyang Wu, and Yong Jae Lee. Visual instruction tuning, 2023b. URL  
 605 <https://arxiv.org/abs/2304.08485>.

606 Yangxiao Lu, Ruosen Li, Liqiang Jing, Jikai Wang, Xinya Du, Yunhui Guo, Nicholas Ruozzi, and  
 607 Yu Xiang. Multimodal reference visual grounding. *arXiv preprint arXiv:2504.02876*, 2025.

608 Tiange Luo, Ang Cao, Gunhee Lee, Justin Johnson, and Honglak Lee. Probing visual language  
 609 priors in VLMs. In Aarti Singh, Maryam Fazel, Daniel Hsu, Simon Lacoste-Julien, Felix  
 610 Berkenkamp, Tegan Maharaj, Kiri Wagstaff, and Jerry Zhu (eds.), *Proceedings of the 42nd In-  
 611 ternational Conference on Machine Learning*, volume 267 of *Proceedings of Machine Learning  
 612 Research*, pp. 41120–41156. PMLR, 13–19 Jul 2025. URL <https://proceedings.mlr.press/v267/luo25b.html>.

613 Tung Minh Luu, Younghwan Lee, Donghoon Lee, Sunho Kim, Min Jun Kim, and Chang D. Yoo.  
 614 Enhancing rating-based reinforcement learning to effectively leverage feedback from large vision-  
 615 language models, 2025. URL <https://arxiv.org/abs/2506.12822>.

616 Chengqi Lyu, Songyang Gao, Yuzhe Gu, Wenwei Zhang, Jianfei Gao, Kuikun Liu, Ziyi Wang,  
 617 Shuaibin Li, Qian Zhao, Haian Huang, Weihan Cao, Jiangning Liu, Hongwei Liu, Junnan Liu,  
 618 Songyang Zhang, Dahua Lin, and Kai Chen. Exploring the limit of outcome reward for learning  
 619 mathematical reasoning, 2025. URL <https://arxiv.org/abs/2502.06781>.

620 Georgios Pantazopoulos and Eda B. Özyigit. Towards understanding visual grounding in visual  
 621 language models, 2025. URL <https://arxiv.org/abs/2509.10345>.

622 Hao Peng, Yunjia Qi, Xiaozhi Wang, Zijun Yao, Bin Xu, Lei Hou, and Juanzi Li. Agentic reward  
 623 modeling: Integrating human preferences with verifiable correctness signals for reliable reward  
 624 systems, 2025a. URL <https://arxiv.org/abs/2502.19328>.

625 Yingzhe Peng, Gongrui Zhang, Miaozen Zhang, Zhiyuan You, Jie Liu, Qipeng Zhu, Kai Yang,  
 626 Xingzhong Xu, Xin Geng, and Xu Yang. Lmm-r1: Empowering 3b lmms with strong reasoning  
 627 abilities through two-stage rule-based rl, 2025b. URL <https://arxiv.org/abs/2503.07536>.

628 Neale Ratzlaff, Man Luo, Xin Su, Vasudev Lal, and Phillip Howard. Training-free mitigation of  
 629 language reasoning degradation after multimodal instruction tuning. In *Proceedings of the AAAI  
 630 Symposium Series*, volume 5, pp. 384–388, 2025.

631 C. E. Shannon. A mathematical theory of communication. *The Bell System Technical Journal*, 27  
 632 (3):379–423, 1948. doi: 10.1002/j.1538-7305.1948.tb01338.x.

633 Rulin Shao, Shuyue Stella Li, Rui Xin, Scott Geng, Yiping Wang, Sewoong Oh, Simon Shaolei Du,  
 634 Nathan Lambert, Sewon Min, Ranjay Krishna, Yulia Tsvetkov, Hannaneh Hajishirzi, Pang Wei  
 635 Koh, and Luke Zettlemoyer. Spurious rewards: Rethinking training signals in rlrv, 2025. URL  
 636 <https://arxiv.org/abs/2506.10947>.

637 Zhihong Shao, Peiyi Wang, Qihao Zhu, Runxin Xu, Junxiao Song, Xiao Bi, Haowei Zhang,  
 638 Mingchuan Zhang, Y. K. Li, Y. Wu, and Daya Guo. Deepseekmath: Pushing the limits of mathe-  
 639 matical reasoning in open language models, 2024. URL <https://arxiv.org/abs/2402.03300>.

648 Haozhan Shen, Peng Liu, Jingcheng Li, Chunxin Fang, Yibo Ma, Jiajia Liao, Qiaoli Shen, Zilun  
 649 Zhang, Kangjia Zhao, Qianqian Zhang, et al. Vlm-r1: A stable and generalizable r1-style large  
 650 vision-language model. *arXiv preprint arXiv:2504.07615*, 2025.

651

652 Qingyi Si, Fandong Meng, Mingyu Zheng, Zheng Lin, Yuanxin Liu, Peng Fu, Yanan Cao, Weiping  
 653 Wang, and Jie Zhou. Language prior is not the only shortcut: A benchmark for shortcut learning in  
 654 vqa. In *Findings of the Association for Computational Linguistics: EMNLP 2022*, pp. 3698–3712,  
 655 2022.

656 Toby Simonds, Kevin Lopez, Akira Yoshiyama, and Dominique Garmier. Rlsr: Reinforcement  
 657 learning from self reward, 2025. URL <https://arxiv.org/abs/2505.08827>.

658

659 Core Team, Zihao Yue, Zhenru Lin, Yifan Song, Weikun Wang, Shuhuai Ren, Shuhao Gu, Shicheng  
 660 Li, Peidian Li, Liang Zhao, Lei Li, Kainan Bao, Hao Tian, Hailin Zhang, Gang Wang, Dawei  
 661 Zhu, Cici, Chenhong He, Bowen Ye, Bowen Shen, Zihan Zhang, Zihan Jiang, Zhixian Zheng,  
 662 Zhichao Song, Zhenbo Luo, Yue Yu, Yudong Wang, Yuanyuan Tian, Yu Tu, Yihan Yan, Yi Huang,  
 663 Xu Wang, Xinzhe Xu, Xingchen Song, Xing Zhang, Xing Yong, Xin Zhang, Xiangwei Deng,  
 664 Wenyu Yang, Wenhan Ma, Weiwei Lv, Weiji Zhuang, Wei Liu, Sirui Deng, Shuo Liu, Shimao  
 665 Chen, Shihua Yu, Shaohui Liu, Shande Wang, Rui Ma, Qiantong Wang, Peng Wang, Nuo Chen,  
 666 Menghang Zhu, Kangyang Zhou, Kang Zhou, Kai Fang, Jun Shi, Jinhao Dong, Jiebao Xiao,  
 667 Jiaming Xu, Huaqiu Liu, Hongshen Xu, Heng Qu, Haochen Zhao, Hanglong Lv, Guoan Wang,  
 668 Duo Zhang, Dong Zhang, Di Zhang, Chong Ma, Chang Liu, Can Cai, and Bingquan Xia. Mimo-vl  
 669 technical report, 2025. URL <https://arxiv.org/abs/2506.03569>.

670

671 Omkar Thawakar, Dinura Dissanayake, Ketan More, Ritesh Thawkar, Ahmed Heakl, Noor Ahsan,  
 672 Yuhao Li, Mohammed Zumri, Jean Lahoud, Rao Muhammad Anwer, et al. Llamav-o1: Rethink-  
 673 ing step-by-step visual reasoning in llms. *arXiv preprint arXiv:2501.06186*, 2025.

674

675 Carel van Niekerk, Renato Vukovic, Benjamin Matthias Ruppik, Hsien chin Lin, and Milica Gašić.  
 676 Post-training large language models via reinforcement learning from self-feedback, 2025. URL  
 677 <https://arxiv.org/abs/2507.21931>.

678

679 Ke Wang, Junting Pan, Weikang Shi, Zimu Lu, Mingjie Zhan, and Hongsheng Li. Measuring multi-  
 680 modal mathematical reasoning with math-vision dataset, 2024. URL <https://arxiv.org/abs/2402.14804>.

681

682 Tengjin Weng, Jingyi Wang, Wenhao Jiang, and Zhong Ming. Visnumbench: Evaluating number  
 683 sense of multimodal large language models, 2025. URL <https://arxiv.org/abs/2503.14939>.

684

685 xAI. Realworldqa: Real-world spatial understanding benchmark. <https://x.ai/blog/grok-1.5v-and-realworldqa>, 2024. CC BY-ND 4.0 license. Benchmark dataset released  
 686 with Grok-1.5 Vision.

687

688 Jiaer Xia, Yuhang Zang, Peng Gao, Yixuan Li, and Kaiyang Zhou. Visionary-r1: Mitigating short-  
 689 cuts in visual reasoning with reinforcement learning, 2025. URL <https://arxiv.org/abs/2505.14677>.

690

691 Tong Xiao, Xin Xu, Zhenya Huang, Hongyu Gao, Quan Liu, Qi Liu, and Enhong Chen. Advancing  
 692 multimodal reasoning capabilities of multimodal large language models via visual perception  
 693 reward, 2025. URL <https://arxiv.org/abs/2506.07218>.

694

695 Guowei Xu, Peng Jin, Ziang Wu, Hao Li, Yibing Song, Lichao Sun, and Li Yuan. Llava-cot: Let  
 696 vision language models reason step-by-step. *arXiv preprint arXiv:2411.10440*, 2024.

697

698 Sihan Yang, Runsen Xu, Yiman Xie, Sizhe Yang, Mo Li, Jingli Lin, Chenming Zhu, Xiaochen  
 699 Chen, Haodong Duan, Xiangyu Yue, Dahua Lin, Tai Wang, and Jiangmiao Pang. Mmsi-bench:  
 700 A benchmark for multi-image spatial intelligence, 2025. URL <https://arxiv.org/abs/2505.23764>.

701

Zijun Yao, Yantao Liu, Yanxu Chen, Jianhui Chen, Junfeng Fang, Lei Hou, Juanzi Li, and Tat-Seng  
 702 Chua. Are reasoning models more prone to hallucination?, 2025. URL <https://arxiv.org/abs/2505.23646>.

702 Tianyu Yu, Haoye Zhang, Qiming Li, Qixin Xu, Yuan Yao, Da Chen, Xiaoman Lu, Ganqu Cui,  
 703 Yunkai Dang, Taiwen He, Xiaocheng Feng, Jun Song, Bo Zheng, Zhiyuan Liu, Tat-Seng Chua,  
 704 and Maosong Sun. Rlaif-v: Open-source ai feedback leads to super gpt-4v trustworthiness, 2024.  
 705 URL <https://arxiv.org/abs/2405.17220>.

706 Weizhe Yuan, Richard Yuanzhe Pang, Kyunghyun Cho, Xian Li, Sainbayar Sukhbaatar, Jing Xu,  
 707 and Jason Weston. Self-rewarding language models, 2025. URL <https://arxiv.org/abs/2401.10020>.

708

710 Xiang Yue, Yuansheng Ni, Kai Zhang, Tianyu Zheng, Ruoqi Liu, Ge Zhang, Samuel Stevens,  
 711 Dongfu Jiang, Weiming Ren, Yuxuan Sun, Cong Wei, Botaao Yu, Ruibin Yuan, Renliang Sun,  
 712 Ming Yin, Boyuan Zheng, Zhenzhu Yang, Yibo Liu, Wenhao Huang, Huan Sun, Yu Su, and  
 713 Wenhua Chen. Mmmu: A massive multi-discipline multimodal understanding and reasoning  
 714 benchmark for expert agi, 2024. URL <https://arxiv.org/abs/2311.16502>.

715 Xiang Yue, Tianyu Zheng, Yuansheng Ni, Yubo Wang, Kai Zhang, Shengbang Tong, Yuxuan Sun,  
 716 Botaao Yu, Ge Zhang, Huan Sun, Yu Su, Wenhua Chen, and Graham Neubig. Mmmu-pro: A more  
 717 robust multi-discipline multimodal understanding benchmark, 2025. URL <https://arxiv.org/abs/2409.02813>.

718

719 Jingyi Zhang, Jiaxing Huang, Huanjin Yao, Shunyu Liu, Xikun Zhang, Shijian Lu, and Dacheng  
 720 Tao. R1-vl: Learning to reason with multimodal large language models via step-wise group  
 721 relative policy optimization, 2025. URL <https://arxiv.org/abs/2503.12937>.

722

723 Renrui Zhang, Dongzhi Jiang, Yichi Zhang, Haokun Lin, Ziyu Guo, Pengshuo Qiu, Aojun Zhou,  
 724 Pan Lu, Kai-Wei Chang, Peng Gao, and Hongsheng Li. Mathverse: Does your multi-modal llm  
 725 truly see the diagrams in visual math problems?, 2024a. URL <https://arxiv.org/abs/2403.14624>.

726

727 Yi-Kai Zhang, Shiyin Lu, Yang Li, Yanqing Ma, Qing-Guo Chen, Zhao Xu, Weihua Luo, Kaifu  
 728 Zhang, De-Chuan Zhan, and Han-Jia Ye. Wings: Learning multimodal llms without text-only  
 729 forgetting. *Advances in Neural Information Processing Systems*, 37:31828–31853, 2024b.

730

731 Xuandong Zhao, Zhewei Kang, Aosong Feng, Sergey Levine, and Dawn Song. Learning to reason  
 732 without external rewards, 2025. URL <https://arxiv.org/abs/2505.19590>.

733

734 Yuze Zhao, Jintao Huang, Jinghan Hu, Xingjun Wang, Yunlin Mao, Daoze Zhang, Zeyinzi Jiang,  
 735 Zhikai Wu, Baole Ai, Ang Wang, Wenmeng Zhou, and Yingda Chen. Swift:a scalable lightweight  
 736 infrastructure for fine-tuning, 2024. URL <https://arxiv.org/abs/2408.05517>.

737

738 Tong Zheng, Lichang Chen, Simeng Han, R Thomas McCoy, and Heng Huang. Learning to reason  
 via mixture-of-thought for logical reasoning. *arXiv preprint arXiv:2505.15817*, 2025.

739

740 Yiyang Zhou, Zhiyuan Fan, Dongjie Cheng, Sihan Yang, Zhaorun Chen, Chenhang Cui, Xiyao  
 741 Wang, Yun Li, Linjun Zhang, and Huaxiu Yao. Calibrated self-rewarding vision language models,  
 742 2024. URL <https://arxiv.org/abs/2405.14622>.

743

744 Yujun Zhou, Zhenwen Liang, Haolin Liu, Wenhao Yu, Kishan Panaganti, Linfeng Song, Dian Yu,  
 745 Xiangliang Zhang, Haitao Mi, and Dong Yu. Evolving language models without labels: Majority  
 746 drives selection, novelty promotes variation. *arXiv preprint arXiv:2509.15194*, 2025.

747

748 Xuekai Zhu, Daixuan Cheng, Dinghuai Zhang, Hengli Li, Kaiyan Zhang, Che Jiang, Youbang Sun,  
 749 Ermo Hua, Yuxin Zuo, Xingtai Lv, Qizheng Zhang, Lin Chen, Fanghao Shao, Bo Xue, Yun-  
 750 chong Song, Zhenjie Yang, Ganqu Cui, Ning Ding, Jianfeng Gao, Xiaodong Liu, Bowen Zhou,  
 751 Hongyuan Mei, and Zhouhan Lin. Flowrl: Matching reward distributions for llm reasoning, 2025.  
 752 URL <https://arxiv.org/abs/2509.15207>.

753

754

755

756 **A APPENDIX**  
757758 **A.1 THE USE OF LARGE LANGUAGE MODELS (LLMs)**  
759760 We acknowledge the use of large language models (LLMs) as assistive tools in this research. Our use  
761 of LLMs was limited to refine grammar and improve language clarity. All outputs from these models  
762 were meticulously reviewed, revised, and verified by the authors, who retain full responsibility for  
763 all content presented in this paper.  
764765 **B EXPERIMENT DETAILS**  
766768 **B.1 PROMPT TEMPLATES**  
769770 This section presents the prompt templates used for constructing the cold start training data and  
771 Model Training prompt. The *See-Think* prompt is used for generating SFT *See-Think* data and  
772 model training. The Caption-Reasoner prompt is used to generate text-only caption reasoner SFT  
773 data and self-reward during training.  
774775 ***See-Think* Prompt Template**  
776777 *{Question}*778 You are tasked with analyzing an image/video to generate a detailed description to help you  
779 answer the question. First analyze the image/video and produce a self-contained descrip-  
780 tion—detailed enough that can lead to the correct answer. Wrap the entire description in  
781 <description></description> tags.782 Next, engage in an internal dialogue and include self-reflection or verification in  
783 your reasoning process. Provide your detailed, step-by-step reasoning based on the  
784 image/video description information and image/video, and enclose this part within  
785 <think></think> tags.  
786787 Finally, provide a single word or phrase answer to the question in \boxed{}.  
788789 The output format should be: <description> image/video description here  
790 </description> <think> reasoning process here </think> \boxed{FINAL  
791 ANSWER here}.792 *Note: {Question} is a placeholder for the actual question.*  
793794 **Caption-Reasoner (Self-Reward) Prompt Template**  
795796 Text description: {Description}  
797800 Question: {Question}  
801802 You are provided a text description of a problem and a question. Determine the an-  
803 swer to the question based on the text description. First provide an internal step-by-step  
804 reasoning within <think></think> tags, then provide a single word or phrase answer  
805 in \boxed{}.  
806807 *Note: {Description} is a placeholder for the actual text caption. {Question} is a  
808 placeholder for the actual question.*  
809

810  
811 Table 5: Through self-reward, the model is implicitly rewarded for text-only reasoning, leading to  
812 improved performance in general reasoning and reduced degradation in math reasoning benchmarks.  
813

Model	MMLU-Pro	SuperGPQA	GSM8K	MATH-500
<i>Backbone model: Qwen2.5-VL-3B</i>				
Before RL	34.3	15.1	78.5	65.2
Vision-R1	47.7	23.1	82.2	66.0
Vision-SR1	48.1	23.2	83.2	68.6
<i>Backbone model: Qwen2.5-VL-7B</i>				
Before RL	33.4	17.1	86.0	73.4
Vision-R1	53.4	26.7	85.5	68.2
Vision-SR1	56.1	26.3	87.6	70.8

### Vision Reasoner (CoT) Prompt Template

821 Question: {Question}  
822

823 You FIRST think about the reasoning process as an internal monologue and then provide  
824 the final answer. The reasoning process MUST BE enclosed within `<think></think>`  
825 tags. The final answer MUST BE put in `\boxed{}`.  
826

827 *Note: {Question} is a placeholder for the actual question.*  
828

### B.2 LLM-AS-A-JUDGE PROMPT

834 We use Gemini-2.5-flash as our LLM-as-a-Judge to evaluate

#### LLM-as-a-Judge Prompt Template

837 • **Model:** Gemini-2.5-flash  
838

#### Prompt Message:

839 Question: {Question}  
840

841 Reference: {Reference}  
842

843 Candidate: {Candidate}  
844

845 You are provided a question, a gold answer, and a candidate answer. Your task is to  
846 judge the correctness of the candidate answer. Return your judgment enclosed with  
847 `<judgment></judgment>`.  
848

849 *Note: {Question} is a placeholder for the actual question; {Reference} is a place-  
850 holder for the gold answer; {Candidate} is a placeholder for the model response.*  
851

#### B.2.1 ANALYSIS ON TEXT-ONLY REASONING

854 An interesting question is how different training strategies affect the text-only reasoning capabilities  
855 of VLMs. In particular, by decoupling visual perception and language reasoning with two separate  
856 rewards, we ask whether these abilities can mutually reinforce one another. To examine this, we  
857 evaluated the text-only performance of VLMs after RL fine-tuning on multimodal data.  
858

859 Specifically, we tested on four text-only datasets: MMLU-Pro and SuperGPQA (multi-disciplinary,  
860 general-domain benchmarks), and MATH-500 and GSM8K (mathematical reasoning tasks). Our  
861 results (Table 5) compare Vision-R1, our method, and pre-RL training baselines.

862 First, we observe that on GSM8K and MATH-500, multimodal RL training, including both Vision-  
863 R1 and our method, degrades text-only reasoning performance. This observation aligns with recent  
864 findings on “text-only forgetting” in VLMs [Zhang et al. \(2024b\)](#); [Ratzlaff et al. \(2025\)](#), which show

Table 6: Results of ablation study: Vision-SR1 v.s. Vision-SR1 w/o visual perception self-reward.

Methods	General Visual Understanding				Visual Math & Hallucination			Avg.
	MMMU -Pro	MMMU	RealWorld QA	VisNum Bench	Math Verse	MATH -Vision	Hallusion Bench	
Vision-SR1 (3B)	40.8	49.6	66.1	41.9	45.8	29.3	68.3	48.8
└ w/o self-reward	40.0	48.0	62.6	41.6	45.1	30.2	65.8	47.6
Vision-SR1 (7B)	<b>40.7</b>	<b>52.2</b>	<b>69.2</b>	<b>43.5</b>	<b>54.5</b>	<b>36.2</b>	<b>68.9</b>	<b>52.2</b>
└ w/o self-reward	42.8	51.8	67.3	35.7	52.6	34.4	67.8	50.3

that visual instruction tuning can impair language reasoning (particularly in mathematics) depending on the underlying LLM. Second, compared to Vision-R1, our method proved more effective at mitigating performance degradation on text-only mathematical benchmarks (MATH-500, GMS8K) and yielded larger gains on general knowledge tasks (MMLU-Pro, SuperGPQA). This indicates that separating the optimization signals for visual perception and language reasoning helps preserve text-only competencies, while still enabling improvements from multimodal training.

## B.2.2 ABLATION STUDY ON SELF-RWARD

We train a control version of our model without the visual reasoning self-reward and Multi-Reward Policy Optimization (Vision-SR1 w/o self-reward). This ablated model still follows a structured output (visual perception, CoT reasoning, and answer) but is optimized only with answer and format rewards. The self-visual reward for self-evaluating visual reasoning and Multi-Reward Policy Optimization are removed. We note the only difference between Vision-SR1 w/o self-reward and Vision-R1 (Huang et al., 2025b) lies in the output structure, i.e., using different system prompts, while all supervision signals (answer reward and format rewards) remain the same. Interestingly, our system prompt yields slightly better performance (+1.0 on average). Table 6 reports the ablation results. We find that not including visual reasoning reward and Multi-Reward Policy Optimization could lead to overall worse VLM task performance compared to including them in the training process.